Development of a novel UHPLC-UV combined with UHPLC-QTOF/MS fingerprint method for the comprehensive evaluation of Nao-Luo-Xin-Tong: multi-wavelength setting based on traditional Chinese medicinal prescription composition

Lina Wang,[1] Yanling Wang,[1] Guangyun Tong,[1] Yu Li[1], Mengnan Lei,[1] Huan Wu,[1] Bin Wang,*[1,2] Rongfeng Hu,*[1,3]

1. Key Laboratory of Xin'an Medicine, Ministry of Education, Anhui University of Chinese Medicine, Hefei, 230038, P. R. China.
2. Institute of pharmaceutical chemistry, Anhui Academy of Chinese Medicine, Hefei, 230038, P. R. China
3. Anhui "115" Xin'an Medicine Research & Development Innovation Team, Anhui Academy of Chinese Medicine, Hefei, 230038, P. R. China

E-mail: wangbin5654@163.com; rongfenghu2003@hotmail.com

Table of contents

	page
Materials and instruments	**2**
Preparation of standard and sample solutions	**2**
UHPLC-UV method	**2**
UHPLC -QTOF/MS method	**2-3**
Investigation of fingerprint methodology	**3**
Figure S1-S3	**4**
Table S1	**4**
Table S2	**5**
Table S3-S4	**6**
Table S5-S7	**7**
Table S8	**8**
Figure S4-S5	**8**
Table S9	**9-11**
Figure S6-S9	**12**
Figure S10-S13	**13**
Figure S14-S17	**14**
Figure S18-S21	**15**
Figure S22-S25	**16**
Figure S26-S30	**17**
Figure S31-S34	**18**
Figure S35-S39	**19**
Figure S40-S44	**20**
Figure S45-S49	**21**

1. Experiments

1.1 Materials and reagents

The four standard substances Hydroxy safflower yellow A, Calycosin-7-O-β-D-glucoside , Ginsenoside Rb_1 and Hypoxanthine were purchased from Shanghai Yuan Ye Biotechnology Co., LTD. The two standard substances Ligustilide and Ferulic acid were purchased from the China Food and Drug Administration. The other two standard substances Notoginsenoside R_1 and Gastrodin were supplied by the China National Institute for the Control of Pharmaceutical and Biological Products and the Maclean Biotechnology Co., LTD., respectively. In addition, the herbals of *Astragali radix*, *Carthamus tinctorius, Panax notoginseng*, *Ligusticum chuanxiong* hort, *Angelicae Sinensis, Gastrodia elata* and *Scolopendra* were all obtained from the pharmacy of Tong Ren Tang. The pure of acetonitrile and methanol was chromatographic grade and the double distilled water was used throughout the course of the experiment.

1.2 Preparation of standard and sample solutions

The stock solutions of Ginsenoside Rb_1, Gastrodin, Hypoxanthine, Hydroxy safflower yellow A, Ferulic acid, Ligustilide, Calycosin-7-O-β-D-glucoside and Notoginsenoside R_1 were prepared with 90% methanol, respectively, and subsequently dilute to scale mark of flask. Finally, the each solutions of 8 kinds of standard substance were obtained at the concentration of 0.69 mg/mL, 0.65 mg/mL, 0.64 mg/mL, 0.72 mg/mL, 0.6 mg/mL, 2.0 mg/mL, 0.57 mg/mL and 0.58 mg/mL, respectively. All the solutions were stored at 4 °C before analysis.

The mixed standards solution were prepared through absorbing abovementioned eight kinds of standard solutions(100 μL) and subsequently placing in the 1 mL volumetric flask, and finally diluting with 90% methanol to the scale.

According to the prescriptions of NLXT: 30.0 g *Astragali radix*, 10.0 g *Carthamus tinctorius,* 4.0 g *Panax notoginseng*, 6 g *Ligusticum chuanxiong* hort, 10.0 g *Gastrodia elata*, 10.0 g *Angelicae Sinensis* and 2.0 g *Scolopendra*, a total 73 g herbs was immersed in 576 mL 75% ethanol. This mixed solution was heated to reflux extraction for 1 hour and then filtered by Buchner funnel. The residue was reflux extracted with 576 mL 75% ethanol again and then filtered. Combine the twice filtered solution and steam until nearly dry, subsequently refrigerate it at -80 ^{o}C for 24 h. After 48 h vacuum freeze drying, the freeze-dried powder of Nao-Luo-Xin-Tong was prepared. Weigh 50 mg the freeze-dried powder in volumetric flask and fix volume to scale using 90% methanol. The solution was ultrasound for 20 min and was filtered with 0.22 μm microporous membrane. Finally, the analysis solution of NLXTD, $\mathbf{S_1}$, was obtained. The other 11 batches sample solutions, $\mathbf{S_2}$ - $\mathbf{S_{12}}$, were prepared according to this method.

1.3 UHPLC -UV method

All samples were performed on an Agilent -Eclipse Plus C_{18} column (2.1 mm × 100 mm, 1.8 μm). The column temperature and the sample chamber temperature were retained at 30 ^{o}C and 10 ^{o}C, respectively. Moreover, the UV wavelength was set at 203 nm, 254 nm, 320 nm and 403 nm, respectively. The mobile phase of **UHPLC** was consisted of A (water containing 0.1% formic acid) and B (acetonitrile), and the gradient was set as follows: 0 - 3 min, 1% B; 4 - 8 min, 3% B; 10 - 12 min, 10% B; 14 - 19 min, 14% B; 20 - 25 min, 18% B; 25 - 48 min, 18% - 35% B; 50 - 55 min, 58% B; 56 - 60 min, 95% B; 61 - 65 min, 1% B. Finally, we obtained the optimal chromatographic results when the flow rate was 0.2 mL/min and sample injection volume was 1 μL.

1.4 UHPLC -QTOF/MS method

The MS analysis was performed on an ACQUITY I-Class **UHPLC** equipment coupled with a Xevo G2-XS QTOF/MS detector (Waters Corp. Milford, MA, USA) via an electrospray interface. The chromatographic separation of all samples was performed on an Eclipse Plus C_{18} column (Agilent Corp.) (dimension 2.1 mm × 100 mm, 1.8 μm particle size). The temperature of column and autosampler were maintained at 30 ^{o}C and 10 ^{o}C, respectively. The **UHPLC** system runs a gradient elution program consisting of water with 0.1% formic acid

(solvent A) and acetonitrile (solvent B). The linear gradient was optimized and was described as follows: 0 - 3 min, 1% B; 4 - 8 min, 3% B; 10 - 12 min, 10% B; 14 - 19 min, 14% B; 20 - 25 min, 18% B; 25 - 48 min, 18% - 35% B; 50 - 55 min, 58% B; 56 - 60 min, 95% B; 61 - 65 min, 1% B, which was delivered at 0.2 mL/min. Mass spectrometry analysis was conducted in positive and negative ion modes. The optimized conditions of QTOF/MS were: capillary voltage, 2.5 kV(ESI+) or 2.0 kV(ESI-); source temperature, 120 ºC (+) or 110 ºC (-); sampling cone, 40 kV; cone gas flow, 50 L/h; desolvation gas temperature and flow rate were 350 ℃ and 600 L/h, respectively; scan range, 50 – 1200 m/z; data acquisition rate, 0.5 s. MSE model was selected for acquisition: the lower collision energy was 10 V, the higher collision ramp energy was 20 – 40 V. To ensure the accuracy, the m/z values of all ions acquired in the QTOF/MS were real-time adjusted by Lock Spray. Leucine-enkephalin was selected as lock mass compound for positive ion mode ($[M+H]^+$: 556.2771) and negative ion mode ($[M-H]^-$: 554.2615).

1.5 Investigation of fingerprint methodology

1.5.1 Precision test: The 1 μL solution of sample $\mathbf{S_1}$ was selected to inject for 6 times. Their chromatograms were recorded and the relative retention time and relative peak area of each common peak were investigated. Taking Hypoxanthine in *Scolopendra* as the reference peak (peak **3**), the results showed the RSD of the relative retention time and the relative peak area were <1.7 and <3.8%, respectively. Thus, the precision of the **UHPLC** is good.

1.5.2 Stability test： The 1 μL solution of sample $\mathbf{S_1}$ was selected to inject at 0, 2, 6, 4, 8, 10, 12 and 24 h. The chromatograms were recorded and the relative retention time and relative peak area of each common peak were investigated. Taking Hypoxanthine in *Scolopendra* as the reference peak (peak **3**), the results showed the RSD of the relative retention time and the relative peak area were <2.0 and <3.2%, respectively. Thus, the stability of the samples $\mathbf{S_1}$ within 24 h is good.

1.5.3 Repeatability test: The 1 μL solution of sample $\mathbf{S_1}$ was selected to inject for 6 times. The chromatograms were recorded and the relative retention time and relative peak area of each common peak were investigated. Taking Hypoxanthine in *Scolopendra* as the reference peak (peak **3**), the results showed the RSD of the relative retention time and the relative peak area were <1.8 and <3.6%, respectively. Thus, the repeatability of method is fine.

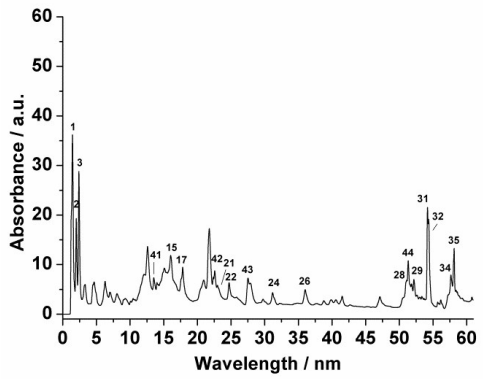

Fig. S1 The common pattern diagram of NLXTD fingerprint chromatograms at 254 nm

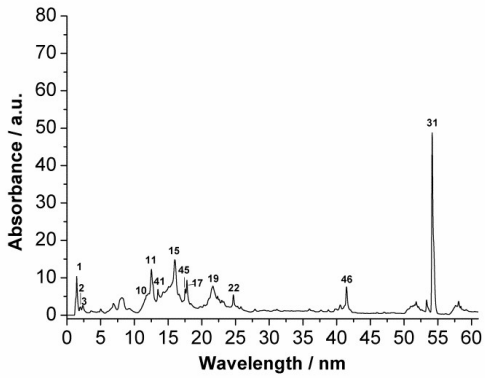

Fig. S2 The common pattern diagram of NLXTD fingerprint chromatograms at 320 nm

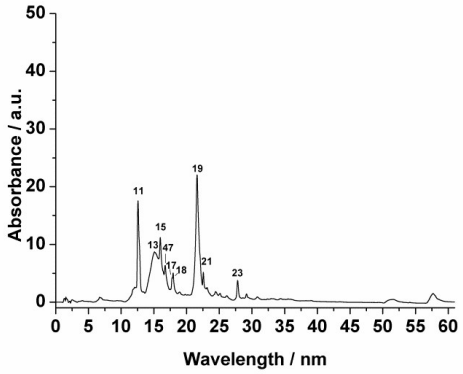

Fig. S3 The common pattern diagram of NLXTD fingerprint chromatograms at 403 nm

Table S1 Investigation of sample preparation with different pretreatment and various solvents for 60 min

Sample pretreatment	Solvents extract	Area of peak **21**	Area of peak **32**
Reflux extraction	75% ethanol	1533	881
Liquid ammonia	/	563	124
Reflux extraction	Petroleum ether	657	389
Reflux extraction	Chloroform	1289	652
Reflux extraction	Methanol	1400	872
Reflux extraction	Acetonitrile	1024	598

Table S2 The data of common peaks of 12 batches NLXTD at 203 nm

Peak	t_R	S1	S2	S3	S4	S5	S6	S7	S8	S9	S10	S11	S12	Contrast	t_R RSD(%)	Area RSD(%)
1	1.38	9135.4	9135.4	9117.0	9218.8	9808.4	9897.1	10830.3	9512.8	9135.4	9086.6	9227.1	9689.7	9482.8	0.10	5.44
2	2.00	903.9	903.9	866.8	897.2	945.8	951.7	1042.6	883.8	903.9	916.4	948.3	1006.7	930.9	0.40	5.52
3	2.37	1109.7	1109.7	1095.1	1078.8	1150.7	1178.0	1328.4	1194.5	1109.7	1125.6	1130.9	1196.2	1150.6	1.01	5.90
4	4.69	129.7	129.7	115.4	124.2	115.6	117.2	127.2	114.9	129.7	181.1	184.4	195.3	138.7	1.33	21.49
5	5.58	55.3	55.3	37.1	35.4	34.7	35.6	56.4	32.8	55.3	50.9	54.4	60.0	46.9	0.99	22.71
6	6.34	472.3	472.3	444.4	421.8	447.0	454.4	515.3	444.3	472.3	453.8	461.6	510.8	464.2	0.76	5.84
7	8.01	155.7	155.7	170.6	175.7	161.4	167.6	192.3	170.3	155.7	163.7	164.7	176.3	167.5	0.81	6.37
8	9.30	152.2	152.2	165.1	162.0	162.7	164.7	188.3	160.3	152.2	140.8	142.9	152.2	158.0	0.70	7.90
9	11.59	297.8	297.8	337.3	325.4	349.8	349.4	368.0	321.6	297.8	257.6	227.7	268.3	308.2	0.24	13.58
10	12.06	381.1	381.1	406.9	409.2	426.8	438.2	484.7	414.1	381.1	350.5	306.4	363.0	395.3	0.09	11.58
11	12.54	550.0	550.0	469.6	478.7	613.7	620.0	680.3	582.3	550.0	518.1	385.4	551.2	545.8	0.16	14.24
12	14.12	141.0	141.0	223.0	141.6	196.7	203.3	214.2	154.9	141.0	159.5	46.3	69.0	152.6	0.22	35.41
13	15.09	162.8	162.8	164.8	160.3	165.4	156.5	181.2	148.2	162.8	181.3	176.3	181.1	167.0	0.27	6.41
14	15.49	64.1	64.1	70.8	68.1	65.4	66.7	77.1	57.3	64.1	65.0	64.2	59.2	65.5	0.22	7.78
15	15.99	346.2	346.2	321.6	322.7	360.7	354.5	404.9	334.6	346.2	352.8	363.8	373.4	352.3	0.13	6.44
16	16.45	85.9	85.9	73.1	82.1	94.5	85.1	102.9	88.4	85.9	86.9	90.8	96.1	88.1	0.07	8.52
17	17.77	180.2	180.2	186.3	290.2	195.4	203.0	363.1	325.0	180.2	171.9	175.1	194.2	220.4	0.21	30.04
18	20.63	84.9	84.9	120.7	131.6	207.2	217.7	225.0	204.7	84.9	125.3	118.9	134.7	145.0	0.27	37.14
19	21.68	174.9	174.9	146.1	152.5	149.1	147.3	134.8	152.7	174.9	177.4	152.7	182.3	160.0	0.17	9.85
20	21.86	231.7	231.7	239.8	232.3	224.0	233.4	207.3	233.7	231.7	220.8	177.7	226.1	224.2	0.16	7.51
21	22.59	1516.2	1516.2	1533.4	1522.1	1649.7	1611.8	1331.2	1653.4	1516.2	1485.5	1225.3	1635.5	1516.4	0.07	8.44
22	24.71	123.2	123.2	130.2	128.1	129.9	168.5	140.8	121.4	123.2	117.5	116.5	124.6	128.9	0.22	10.9
23	27.88	154.4	154.4	167.6	158.3	137.5	145.1	152.7	137.8	154.4	153.8	145.2	148.1	150.8	0.21	5.69
24	32.21	124.4	124.4	91.2	104.3	94.9	100.5	168.0	151.3	124.4	115.4	120.8	139.4	121.6	0.06	18.88
25	34.01	249.5	249.5	353.3	356.1	318.6	318.7	358.2	323.3	249.5	240.7	247.2	269.5	294.5	0.08	16.23
26	36.08	260.0	260.0	274.7	267.0	190.5	184.0	213.1	189.7	260.0	254.4	244.1	272.6	239.2	0.08	14.51
27	45.83	150.7	150.7	156.3	157.3	112.6	109.1	125.3	107.8	150.7	153.8	148.3	169.2	141.0	0.09	15.07
28	50.99	169.7	169.7	258.6	252.0	59.3	62.6	65.8	121.2	169.7	206.3	199.1	196.8	160.9	0.02	43.33
29	52.17	323.6	323.6	505.8	505.6	146.4	141.1	147.7	134.5	323.6	461.2	416.3	333.4	313.6	0.01	45.52
30	52.57	180.6	180.6	307.8	304.9	72.2	69.1	72.3	70.2	180.6	282.3	245.1	183.9	179.1	0.02	51.67
31	54.18	595.8	595.8	596.3	637.4	205.4	200.4	217.0	215.0	595.8	679.0	594.4	661.7	482.8	0.01	42.22
32	54.30	638.5	638.5	895.7	847.4	275.6	260.8	277.7	269.1	638.5	705.5	615.4	640.9	558.6	0.03	41.08
33	57.27	202.7	202.7	334.6	347.5	139.0	144.1	143.9	137.7	202.7	331.2	313.5	340.8	236.7	0.01	37.68
34	57.65	33.9	33.9	268.1	276.3	136.9	153.0	132.9	135.2	33.9	276.6	293.8	316.3	174.2	0.01	62.0
35	58.04	354.8	354.8	554.5	556.4	353.0	357.0	350.2	355.8	354.8	507.2	481.9	524.4	425.4	0.01	21.13
36	58.39	68.1	68.1	90.2	92.0	69.6	74.4	68.4	78.8	68.1	117.6	112.9	114.6	85.2	0.02	23.22
37	58.77	40.2	40.2	46.2	45.9	13.6	12.2	14.3	12.7	40.2	48.8	38.1	38.5	32.6	0.01	45.05
38	58.94	868.9	868.9	982.5	992.4	292.8	278.5	327.6	286.9	868.9	958.3	847.6	878.3	704.3	0.01	43.32
39	59.45	88.9	88.9	97.2	96.6	25.5	26.3	39.5	26.0	88.9	119.7	108.2	90.5	74.7	0.01	46.68
40	59.72	1702.8	1702.8	1945.1	1941.5	586.7	544.0	612.6	557.2	1702.8	1884.6	1682.1	1767.6	1385.8	0.02	43.72

Table S3 The data of common peaks of 12 batches NLXTD at 254 nm

Peak	t_R	S1	S2	S3	S4	S5	S6	S7	S8	S9	S10	S11	S12	Contrast	t_R RSD(%)	Area RSD(%)
1	1.40	453.7	559.3	662.2	658.5	703.8	714.3	712.7	663.8	638.8	640.8	643.8	677.4	644.1	0.36	11.34
2	2.01	133.6	216.0	211.0	202.8	224.4	248.8	235.2	227.1	226.0	226.5	214.9	238.7	217.1	1.03	13.42
3	2.39	325.5	336.3	331.7	331.9	361.2	417.8	368.1	364.8	348.7	352.2	364.1	396.0	358.2	0.96	7.64
41	13.52	35.9	33.6	33.1	33.3	37.5	35.8	36.5	33.1	30.3	32.3	34.0	36.5	34.3	0.21	6.16
15	16.03	267.1	182.7	135.4	89.2	222.7	95.0	139.1	129.7	130.8	138.6	115.4	125.0	147.6	0.21	35.26
17	17.81	144.0	141.6	142.8	141.0	153.5	152.5	149.8	144.0	112.0	113.9	110.9	117.4	135.3	0.22	12.29
42	22.36	39.5	40.6	16.9	17.4	17.4	17.5	58.7	33.7	33.8	52.9	33.3	30.0	32.6	0.16	42.87
21	22.56	87.7	88.2	52.4	53.0	54.4	55.2	109.6	75.4	74.4	110.0	77.1	58.3	74.6	0.11	28.14
22	24.70	218.5	61.3	70.1	67.1	58.8	64.7	61.7	64.8	67.3	68.5	45.9	45.8	74.5	0.26	61.77
43	27.51	100.8	108.2	107.9	112.6	32.7	38.1	40.9	43.2	132.6	133.2	128.8	137.6	93.1	0.20	44.87
24	31.17	70.3	72.2	70.8	71.4	62.5	61.9	63.2	61.7	68.4	66.7	66.3	69.4	67.1	0.21	5.84
26	36.00	102.5	105.0	102.9	103.7	66.0	64.3	64.3	63.9	93.8	96.1	91.7	97.6	87.7	0.14	19.95
28	51.09	119.5	116.0	114.1	113.8	74.9	71.4	75.0	72.9	32.5	34.9	31.3	33.4	74.1	0.06	47.69
44	51.31	159.6	157.4	154.3	157.3	89.0	84.4	87.2	84.6	141.4	151.1	137.2	149.2	129.4	0.01	25.1
29	52.15	45.9	45.5	44.9	44.4	27.5	25.8	26.3	25.5	37.7	41.2	35.6	38.3	36.6	0.01	22.6
31	54.18	230.6	254.6	255.5	262.3	80.7	80.3	85.8	85.3	282.2	317.3	278.5	310.2	210.3	0.02	46.07
32	54.34	351.9	348.3	343.5	339.7	106.2	96.0	98.2	94.4	259.7	293.4	245.5	261.6	236.5	0.04	45.68
34	57.65	173.6	161.0	160.3	160.7	96.9	115.3	113.9	111.4	190.4	202.8	172.7	200.9	155.0	0.01	23.78
35	58.13	243.7	210.7	208.1	210.5	69.0	82.7	85.3	79.1	186.9	206.4	194.3	194.7	164.3	0.01	39.31

Table S4 The data of common peaks of 12 batches NLXTD at 320 nm

Peak	t_R	S1	S2	S3	S4	S5	S6	S7	S8	S9	S10	S11	S12	Contrast	t_R RSD(%)	Area RSD(%)
1	1.41	168.0	166.3	161.1	165.1	178.1	178.9	182.4	171.7	165.6	176.9	179.3	188.0	173.5	0.08	4.78
2	1.99	28.8	27.8	27.5	28.3	31.2	31.5	32.0	30.8	29.4	19.4	20.9	22.2	27.5	0.30	15.70
3	2.35	50.2	55.3	51.5	51.1	52.5	61.3	62.1	57.8	46.4	46.2	42.7	60.2	53.1	0.68	11.95
10	12.14	171.0	176.3	166.8	71.7	77.8	78.1	77.2	68.2	65.1	66.9	67.4	69.3	96.3	0.36	47.26
11	12.53	240.3	238.6	233.4	239.9	257.4	249.4	252.7	231.5	219.7	223.2	232.4	253.4	239.3	0.19	5.03
41	13.49	27.7	27.4	24.9	29.2	31.3	35.9	39.7	39.7	39.3	37.0	40.1	41.5	34.5	0.24	17.34
15	16.00	264.0	273.5	439.3	277.4	410.5	262.3	257.2	268.5	463.7	284.6	289.4	314.6	317.1	0.36	23.72
45	17.54	46.8	48.0	48.2	47.1	51.0	50.8	49.5	48.4	45.9	45.7	44.2	40.0	47.1	0.20	6.40
17	17.78	102.1	102.2	102.8	102.0	108.1	105.9	104.4	104.6	102.2	105.2	104.3	107.8	104.3	0.23	2.07
19	21.64	228.1	225.4	204.5	211.4	202.7	199.2	198.4	133.8	208.8	204.7	202.6	199.6	201.6	0.22	11.63
22	24.68	45.6	44.1	44.0	45.9	42.2	44.4	58.3	43.2	44.1	44.2	42.3	75.9	47.8	0.26	20.47
46	41.46	175.8	175.4	173.8	171.1	61.9	57.2	59.0	47.7	121.2	144.0	117.0	134.1	119.9	0.09	42.64
31	54.16	1131.5	1161.5	1156.2	1149.0	360.0	342.4	356.9	349.2	974.5	1092.3	946.6	1050.9	839.3	0.02	43.61

Table S5 The data of common peaks of 12 batches NLXTD at 403 nm

Peak	t_R	S1	S2	S3	S4	S5	S6	S7	S8	S9	S10	S11	S12	Contrast	t_R RSD(%)	Area RSD(%)
11	12.57	408.6	401.6	390.1	396.9	439.0	435.9	440.4	259.6	396.0	396.6	405.8	373.1	395.3	0.14	12.03
13	15.09	178.2	187.1	507.3	165.4	195.6	566.4	567.0	536.7	184.2	501.1	509.5	654.4	396.1	0.20	48.77
15	15.98	73.1	71.0	244.1	65.3	73.7	277.0	278.5	258.1	63.1	251.1	253.0	316.3	185.4	0.11	56.20
47	16.73	35.3	32.9	88.4	31.2	32.0	95.9	99.4	92.2	35.4	94.7	97.8	120.7	71.3	0.12	48.26
17	17.79	20.9	19.5	18.3	18.5	17.8	18.0	19.4	18.0	18.0	17.2	17.6	21.2	18.7	0.06	6.86
48	17.94	50.5	49.2	45.9	45.2	49.1	48.8	47.2	44.4	43.9	42.5	41.8	48.7	46.4	0.05	6.22
19	21.60	699.8	699.1	669.2	682.9	861.1	848.3	852.9	799.8	704.4	735.2	750.0	872.5	764.6	0.13	10.13
21	22.56	27.7	27.6	28.1	27.6	47.6	47.2	50.1	47.2	29.8	70.3	71.2	33.6	42.3	0.04	37.95
23	27.81	59.8	57.6	56.7	56.1	56.2	55.4	56.3	54.5	54.7	55.1	54.9	68.9	57.2	0.07	6.94

Table S6 The similarity results of 12 batches of **NLXTD** at 250 nm

Peak	S1	S2	S3	S4	S5	S6	S7	S8	S9	S10	S11	S12	Contrast
1	1	0.92	0.863	0.847	0.723	0.693	0.611	0.787	0.866	0.874	0.851	0.861	0.887
2	0.92	1	0.953	0.934	0.774	0.767	0.681	0.896	0.926	0.919	0.928	0.916	0.951
3	0.863	0.953	1	0.985	0.822	0.827	0.785	0.876	0.905	0.876	0.906	0.889	0.957
4	0.847	0.934	0.985	1	0.82	0.829	0.775	0.868	0.901	0.88	0.904	0.895	0.953
5	0.723	0.774	0.822	0.82	1	0.972	0.921	0.848	0.78	0.77	0.793	0.79	0.894
6	0.693	0.767	0.827	0.829	0.972	1	0.942	0.858	0.798	0.778	0.812	0.802	0.9
7	0.611	0.681	0.785	0.775	0.921	0.942	1	0.769	0.716	0.688	0.725	0.7	0.832
8	0.787	0.896	0.876	0.868	0.848	0.858	0.769	1	0.922	0.905	0.937	0.917	0.947
9	0.866	0.926	0.905	0.901	0.78	0.798	0.716	0.922	1	0.981	0.988	0.984	0.965
10	0.874	0.919	0.876	0.88	0.77	0.778	0.688	0.905	0.981	1	0.978	0.991	0.954
11	0.851	0.928	0.906	0.904	0.793	0.812	0.725	0.937	0.988	0.978	1	0.981	0.968
12	0.861	0.916	0.889	0.895	0.79	0.802	0.7	0.917	0.984	0.991	0.981	1	0.961

Table S7 The similarity results of 12 batches of **NLXTD** at 320 nm

Peak	S1	S2	S3	S4	S5	S6	S7	S8	S9	S10	S11	S12	Contrast
1	1	0.993	0.983	0.988	0.772	0.799	0.826	0.831	0.955	0.978	0.971	0.978	0.981
2	0.993	1	0.984	0.992	0.77	0.797	0.808	0.814	0.948	0.971	0.963	0.965	0.976
3	0.983	0.984	1	0.98	0.815	0.81	0.819	0.831	0.972	0.966	0.963	0.961	0.981
4	0.988	0.992	0.98	1	0.777	0.802	0.813	0.82	0.957	0.979	0.972	0.97	0.98
5	0.772	0.77	0.815	0.777	1	0.96	0.903	0.905	0.876	0.803	0.834	0.798	0.866
6	0.799	0.797	0.81	0.802	0.96	1	0.935	0.924	0.884	0.845	0.877	0.836	0.889
7	0.826	0.808	0.819	0.813	0.903	0.935	1	0.992	0.858	0.825	0.85	0.882	0.893
8	0.831	0.814	0.831	0.82	0.905	0.924	0.992	1	0.87	0.831	0.855	0.89	0.899
9	0.955	0.948	0.972	0.957	0.876	0.884	0.858	0.87	1	0.981	0.987	0.965	0.987
10	0.978	0.971	0.966	0.979	0.803	0.845	0.825	0.831	0.981	1	0.997	0.978	0.985
11	0.971	0.963	0.963	0.972	0.834	0.877	0.85	0.855	0.987	0.997	1	0.976	0.989

12	0.978	0.965	0.961	0.97	0.798	0.836	0.882	0.89	0.965	0.978	0.976	1	0.985

Table S8 The similarity results of 12 batches of **NLXTD** at 403 nm

Peak	S1	S2	S3	S4	S5	S6	S7	S8	S9	S10	S11	S12	Contrast
1	1	0.931	0.922	0.924	0.998	0.937	0.938	0.909	0.923	0.935	0.935	0.906	0.97
2	0.931	1	0.926	0.911	0.998	0.94	0.941	0.913	0.933	0.938	0.939	0.91	0.973
3	0.922	0.926	1	0.917	0.912	0.998	0.998	0.985	0.923	0.998	0.998	0.995	0.986
4	0.924	0.911	0.917	1	0.998	0.933	0.934	0.904	0.917	0.93	0.931	0.901	0.968
5	0.998	0.998	0.912	0.998	1	0.931	0.931	0.909	0.999	0.927	0.928	0.901	0.966
6	0.937	0.94	0.998	0.933	0.931	1	0.951	0.991	0.938	0.999	0.999	0.996	0.993
7	0.938	0.941	0.998	0.934	0.931	0.951	1	0.991	0.939	0.999	0.999	0.995	0.994
8	0.909	0.913	0.985	0.904	0.909	0.991	0.991	1	0.912	0.988	0.988	0.996	0.98
9	0.923	0.933	0.923	0.917	0.999	0.938	0.939	0.912	1	0.935	0.936	0.908	0.971
10	0.935	0.938	0.998	0.93	0.927	0.999	0.999	0.988	0.935	1	0.926	0.994	0.992
11	0.935	0.939	0.998	0.931	0.928	0.999	0.999	0.988	0.936	0.926	1	0.994	0.992
12	0.906	0.91	0.995	0.901	0.901	0.996	0.995	0.996	0.908	0.994	0.994	1	0.981

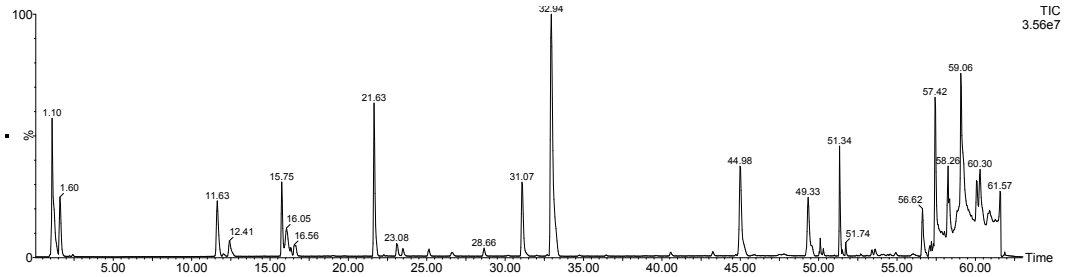

Fig. S4 The QTOF/MS-TIC of NLXTD extracts in negative ion mode

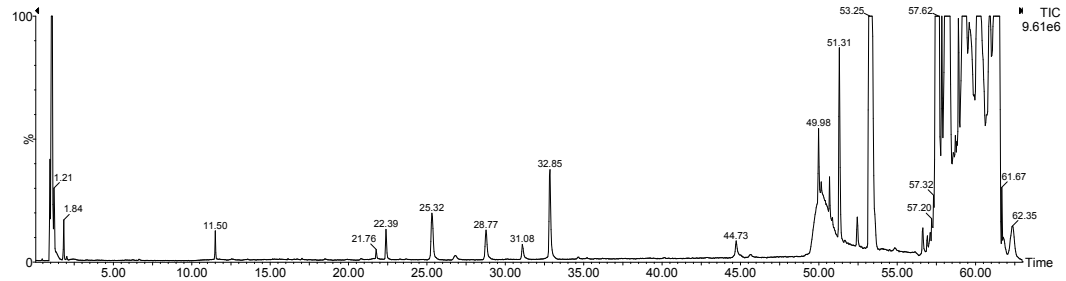

Fig. S5 The QTOF/MS-TIC of NLXTD extracts in positive ion mode

Table S9 UHPLC-tof /MS^n data and identification of compounds in NLXTD

No.	t_R(min)	Identification	Formula	Cal. m/z $[M-H]^-/[M-HCOO]^-$	Cal. m/z $[M+H]^+/[M+Na]^+$	Ref.
1	1.14	Valine	$C_5H_{11}NO_2$	/	118.0876	15d
2	1.16	L- Pyroglutamic acid	$C_5H_7NO_3$	128.0352	130.0503	13d
3	1.21	Proline	$C_5H_9NO_2$	/	116.0709	15d
4	1.22	Thymine **(Peak 1)**	$C_5H_6N_2O_2$	/	127.0511	15c
5	2.17	Uridine **(Peak 2)**	$C_9H_{12}N_2O_6$	243.0614	/	15c
6	2.30	Citric acid	$C_6H_8O_7$	191.0182	215.0171	13d
7	2.33	Hypoxanthine **(Peak 3)**	$C_5H_4N_4O$	135.0308	137.0456	15a,b
8	2.40	3-[6-O-(D-galactopyranosyl)-β-galactopyranosyl]oxy-1,2-propan-ediyl diacetate	$C_{19}H_{32}O_{15}$	499.1647	501.1814	10a
9	6.15	Gastrodin **(Peak 6)**	$C_{13}H_{18}O_7$	331.1041	/	13a,d
10	11.40	Jineol	$C_9H_7NO_2$	160.0408	162.0555	15a,b
11	11.50	Tryptophan	$C_{11}H_{12}N_2O_2$	203.0816	205.0963	14a
12	11.55	Hydroxy safflower yellow A **(Peak 9)**	$C_{27}H_{32}O_{16}$	611.1629	613.1791	10b
13	12.50	Parishin E **(Peak 11)**	$C_{19}H_{24}O_{13}$	459.1147	/	13b,d
14	12.60	6-Hydroxykaempferol -3, 6-O-7-O-glucuronide	$C_{33}H_{38}O_{23}$	801.1727	803.1897	10c
15	13.38	Chlorogenic acid **(Peak 41)**	$C_{16}H_{18}O_9$	353.0878	/	14a
16	14.48	p-Hydroxybenzaldehyde	$C_7H_6O_2$	121.0298	/	13b,c
17	15.09	Ferulic acid **(Peak 13)**	$C_{10}H_{10}O_4$	193.0487	/	14a
18	15.11	Notoginsenoside J **(Peak 14)**	$C_{42}H_{74}O_{16}$	879.4968	/	11a
19	16.28	Parishin B **(Peak 15)**	$C_{32}H_{40}O_{19}$	727.2070	/	13a,d
20	16.67	Kaempferol-3-O-rutinoside **(Peak 16)**	$C_{27}H_{30}O_{15}$	593.1511	595.1666	10b
21	16.72	6-Hydroxyapigenin 3-O-Rutinoside -6-O-glucoside **(Peak 47)**	$C_{33}H_{40}O_{21}$	771.1941	773.2084	10c
22	16.99	6-Hydroxykaempferol 3,6-diglucoside	$C_{27}H_{30}O_{17}$	625.1389	627.1542	10d
23	17.11	Parishin **(Peak 45)**	$C_{32}H_{40}O_{19}$	727.2070	/	13a,d
24	17.39	6-Hydroxyapigenin 6-O-glucoside -7-O-glucuronide **(Peak 17)**	$C_{27}H_{28}O_{17}$	/	625.1422	10a

25	19.16	Rutin	$C_{27}H_{30}O_{16}$	609.1461	611.1594	10b
26	19.83	Quercetin-7-O- glucuronide	$C_{21}H_{21}O_{12}$	463.0870	465.1041	10c
27	20.77	Calycosin-7-O-β- D-glucoside **(Peak 18)**	$C_{22}H_{22}O_{10}$	491.1187	447.1294	9a
28	21.50	6-Hydroxykaempferol 3-β-rutinoside	$C_{27}H_{30}O_{16}$	609.1461	611.1594	10a
29	21.75	Parishin A **(Peak 19)**	$C_{45}H_{56}O_{25}$	995.3002	/	13a
30	21.78	Disubstituted parishin	$C_{32}H_{40}O_{19}$	727.2070	/	13a
31	21.80	Tinctormin **(Peak 20)**	$C_{27}H_{31}NO_{14}$	592.1697		10f
32	22.07	6-Hydroxykaempferol 3-β- glucoside **(Peak 42)**	$C_{21}H_{21}O_{12}$	463.0870	465.1041	10b
33	23.17	Safflor yellow B	$C_{48}H_{52}O_{26}$	1043.2640	1045.2800	10b
34	22.37	Cyclocephaloside A **(Peak 21)**	$C_{37}H_{60}O_{10}$	663.3949	/	9b
35	23.65	Safflor yellow A/ Kaempferol-3-O-rutinoside	$C_{27}H_{30}O_{15}$	593.1511	595.1666	10b
36	24.58	Cynaroside **(Peak 22)**	$C_{21}H_{20}O_{11}$	447.0969		10b
37	26.55	Safflor yellow C	$C_{27}H_{29}NO_{13}$	574.1577		10a
38	26.57	4-Hydroxy-3-butylphthalide	$C_{12}H_{14}O_3$	205.0871	207.1024	12a
39	26.64	Senkyunolide I/H	$C_{12}H_{16}O_4$	/	247.0945	12a
40	26.80	Senkyunolide F/ 4-Hydroxy-3-butylphthalide	$C_{12}H_{14}O_3$	205.0871	207.1024	14a
41	27.82	Biochanin-A **(Peak 23)**	$C_{16}H_{12}O_5$	283.0599	285.0750	9a
42	29.96	Ginseng saponin Ro	$C_{48}H_{76}O_{19}$	1007.5458	/	11b
43	30.03	Notoginsenoside R_3	$C_{48}H_{82}O_{19}$	1007.5458	/	11c
44	30.06	Ononin	$C_{22}H_{22}O_9$	475.1246	431.1343	9a
45	32.07	Notoginsenoside R_1 **(Peak 24)**	$C_{47}H_{80}O_{18}$	977.5295	/	11c
46	32.77	Ginseng saponin Rg_1/Rf/ F_{11}	$C_{42}H_{72}O_{14}$	845.4889		11c
47	32.94	Notoginsenoside K/ Ginseng saponin Rd/Re	$C_{48}H_{82}O_{18}$	991.5464	947.5539	11a
48	32.953	Ginseng saponin Rh_4	$C_{36}H_{60}O_8$	/	621.4340	11c
49	34.15	Malonyl ginsenosides Rg_1 **(Peak 25)**	$C_{45}H_{74}O_{17}$	885.4907	/	11a
50	36.12	Formononetin **(Peak 26)**	$C_{16}H_{12}O_4$	267.0661	269.0810	9a
51	37.59	Methylnissolin	$C_{17}H_{16}O_5$	299.0903	/	9b
52	40.97	Odoratin	$C_{17}H_{14}O_6$	313.0735	337.0695	9a
53	41.40	Senkyunolide D **(Peak 46)**	$C_{12}H_{14}O_4$	221.0805	/	12a
54	42.88	Notoginsenoside Rw_1	$C_{46}H_{78}O_{17}$	947.5198		11a
55	42.98	Notoginsenoside H	$C_{47}H_{80}O_{19}$	947.5198		11a

56	44.38	Ginseng saponin F_2/ Rg_2/ Rg_3	$C_{42}H_{72}O_{13}$	829.4936	/	11c
57	44.58	Ginseng saponin Rh_1/ F_1	$C_{36}H_{62}O_9$	683.4356	/	11c
58	44.76	Ginseng saponin Rk_1/Rg_1	$C_{42}H_{70}O_{12}$	/	767.4960	11c
29	45.76	Ginseng saponin Rb_1 **(Peak 27)**	$C_{54}H_{92}O_{23}$	1153.6025	1109.6073	11c
60	46.96	Senkyunolide F	$C_{12}H_{14}O_3$	205.0871	/	12a
61	50.40	Notoginsenoside Fd/Fe	$C_{47}H_{80}O_{17}$	961.5364	/	11c
62	50.96	Soyasaponin Ⅰ **(Peak 29)**	$C_{48}H_{78}O_{18}$	987.5231	/	9b
63	51.31	Senkyunolide A **(Peak 44)**	$C_{12}H_{16}O_2$	/	193.1201	14a
64	52.48	Ligustilide **(Peak 30)**	$C_{12}H_{14}O_2$	/	191.1068	14a
65	53.07	Sedanolide	$C_{12}H_{18}O_2$	/	195.1383	12a
66	54.25	Butylphthalide **(Peak 31)**	$C_{12}H_{14}O_2$	/	191.1068	14a
67	54.50	3-Butylidenephthalide **(Peak 32)**	$C_{12}H_{12}O_2$	/	189.0899	12a
68	57.24	Levistilide A **(Peak 33)**	$C_{24}H_{28}O_4$	379.1894	/	12a
69	57.59	Butylidenephthalide **(Peak 34)**	$C_{12}H_{12}O_2$	/	189.0899	14a
70	58.02	Stearic acid **(Peak 35)**	$C_{18}H_{36}O_2$	283.2630	/	15d
71	59.06	Linoleic acid **(Peak 38)**	$C_{18}H_{32}O_2$	279.2307	/	14b
72	59.20	Oleic acid **(Peak 39)**	$C_{18}H_{34}O_2$	281.2484	282.2702	15d

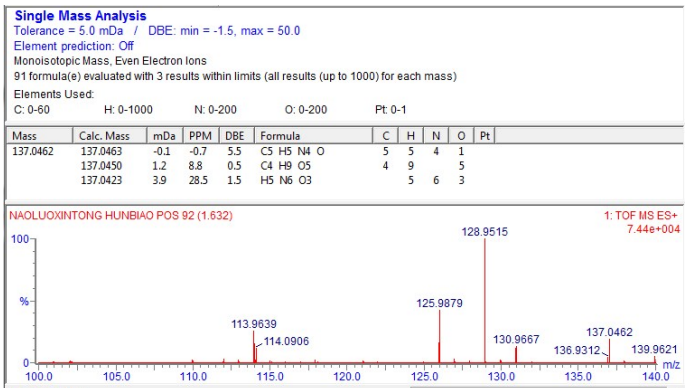

Fig. S6 The analysis of elemental composition about m/z 137.0462 (Peak **3**)

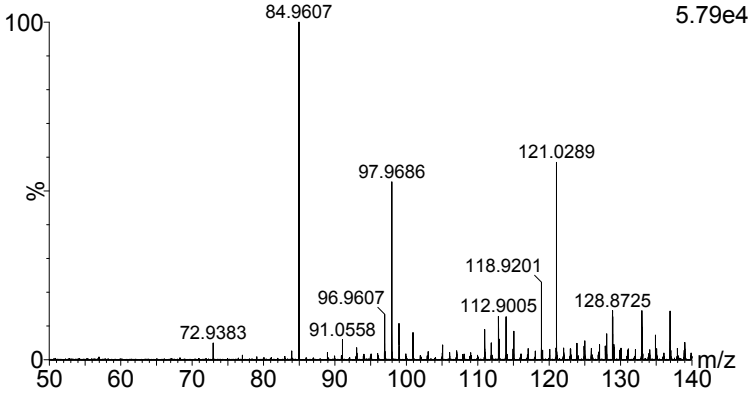

Fig. S7 MS fragmentation for the m/z 137.0462 (Peak **3**)

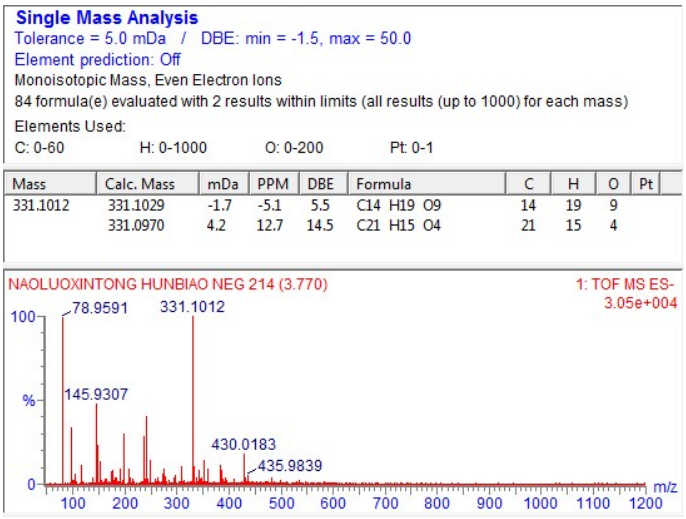

Fig. S8 The analysis of elemental composition about m/z 331.1012 (Peak **6**)

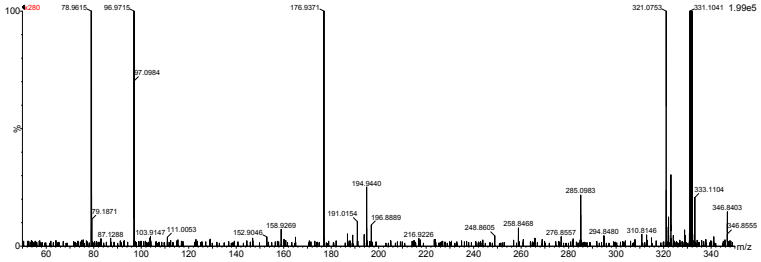

Fig. S9 MS fragmentation for the m/z 331.1012 (Peak **6**)

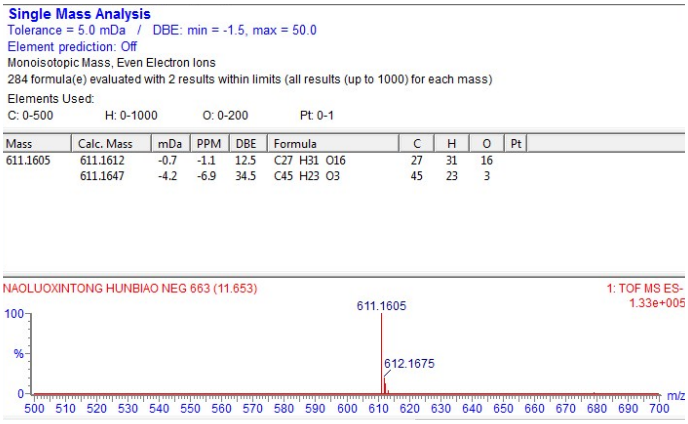

Fig. S10 The analysis of elemental composition about m/z 611.1605 (Peak **9**)

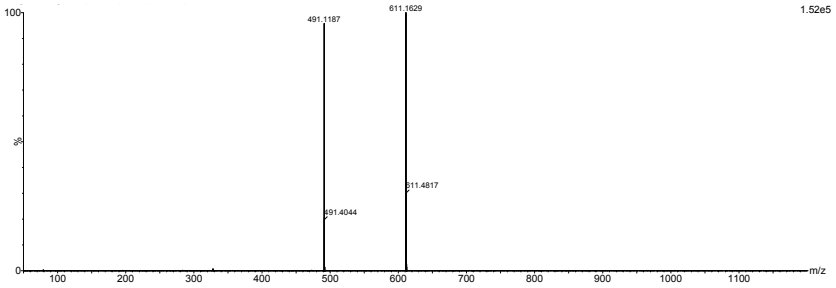

Fig. S11 MS fragmentation for the m/z 611.1605 (Peak **9**)

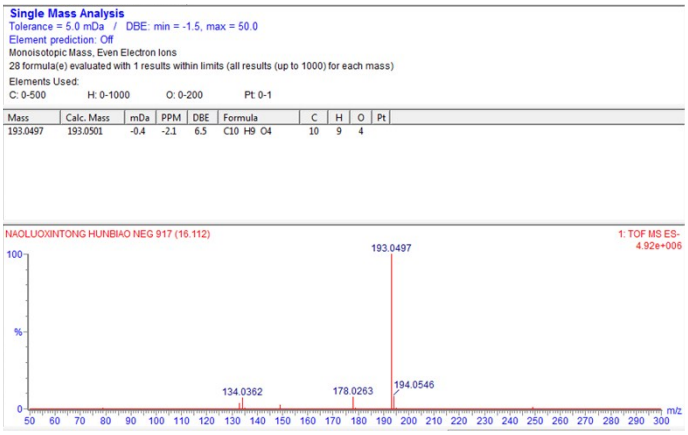

Fig. S12 The analysis of elemental composition about m/z 611.1605 (Peak **13**)

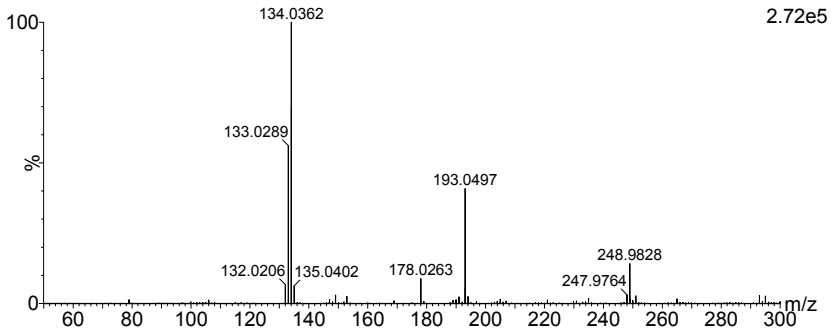

Fig. S13 MS fragmentation for the m/z 611.1605 (Peak **13**)

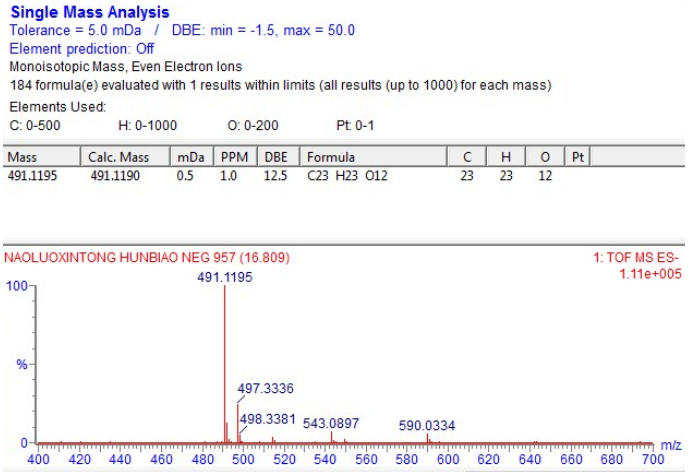

Fig. S14 The analysis of elemental composition about m/z 491.1195 (Peak **18**)

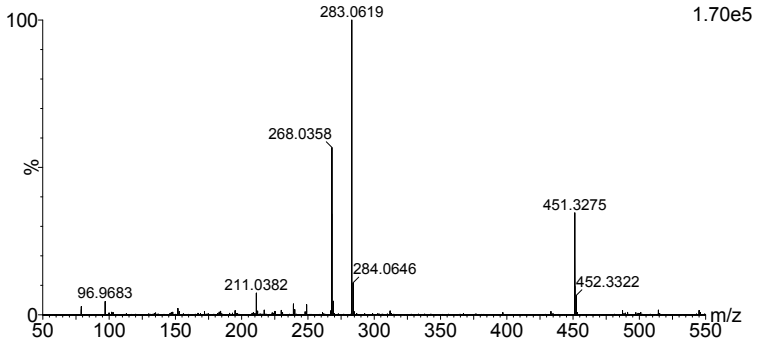

Fig. S15 MS fragmentation for the m/z 491.1195 (Peak **18**)

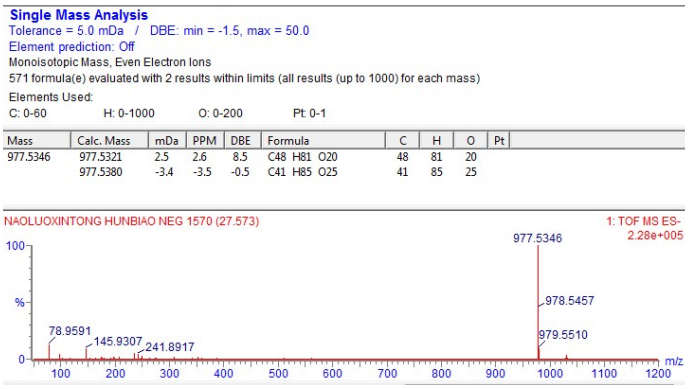

Fig. S16 The analysis of elemental composition about m/z 977.5346 (Peak **24**)

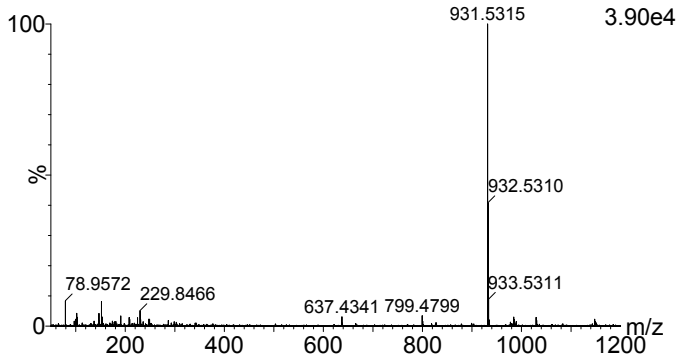

Fig. S17 MS fragmentation for the m/z 977.5346 (Peak **24**)

Single Mass Analysis
Tolerance = 5.0 mDa / DBE: min = -1.5, max = 50.0
Element prediction: Off
Monoisotopic Mass, Even Electron Ions
599 formula(e) evaluated with 2 results within limits (all results (up to 1000) for each mass)
Elements Used:
C: 0-60 H: 0-1000 O: 0-200 Pt: 0-1

Mass	Calc. Mass	mDa	PPM	DBE	Formula	C	H	O	Pt
1153.6031	1153.6006	2.5	2.2	9.5	C55 H93 O25	55	93	25	
	1153.6065	-3.4	-2.9	0.5	C48 H97 O30	48	97	30	

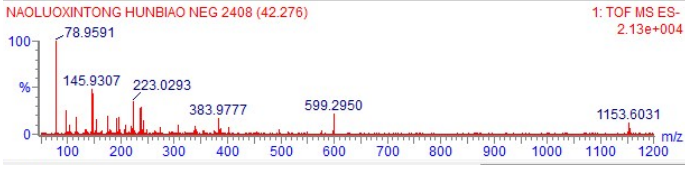

Fig. S18 The analysis of elemental composition about m/z 1153.6031 (Peak **27**)

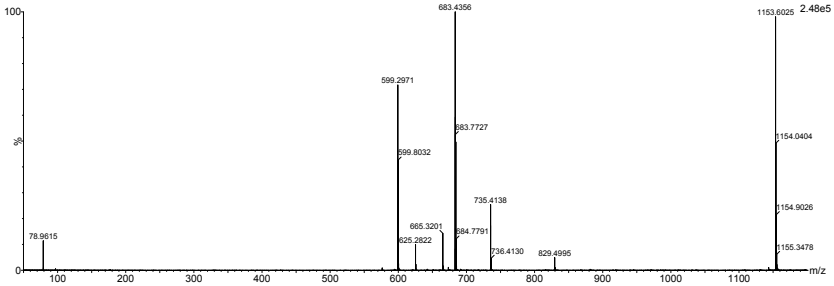

Fig. S19 MS fragmentation for the m/z 1153.6031 (Peak **27**)

Single Mass Analysis
Tolerance = 5.0 mDa / DBE: min = -1.5, max = 50.0
Element prediction: Off
Monoisotopic Mass, Even Electron Ions
28 formula(e) evaluated with 1 results within limits (all results (up to 1000) for each mass)
Elements Used:
C: 0-60 H: 0-1000 O: 0-200 Pt: 0-1

Mass	Calc. Mass	mDa	PPM	DBE	Formula	C	H	O	Pt
191.1078	191.1072	0.6	3.1	5.5	C12 H15 O2	12	15	2	

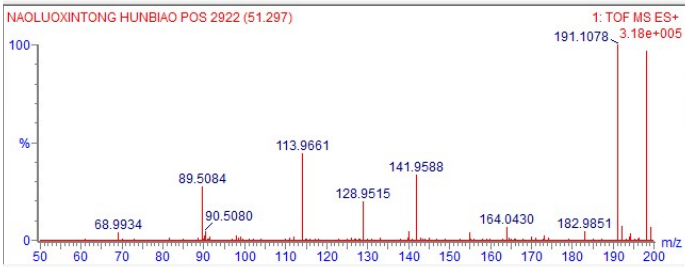

Fig. S20 The analysis of elemental composition about m/z 191.1078 (Peak **30**)

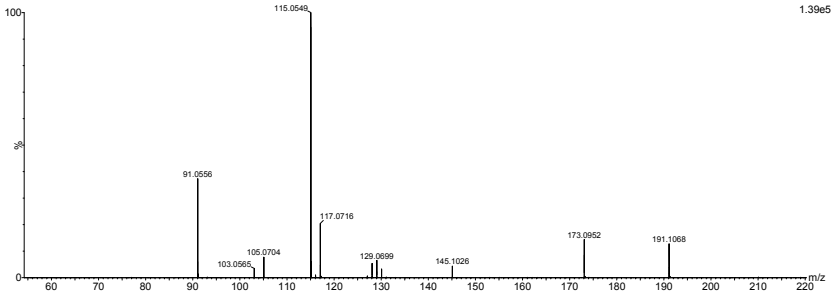

Fig. S21 MS fragmentation for the m/z 191.1078 (Peak **30**)

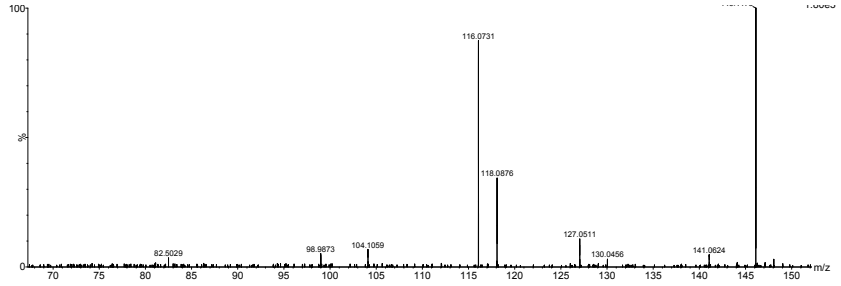

Fig. S22 MS fragmentation for the m/z 127.0511 (Peak **1**)

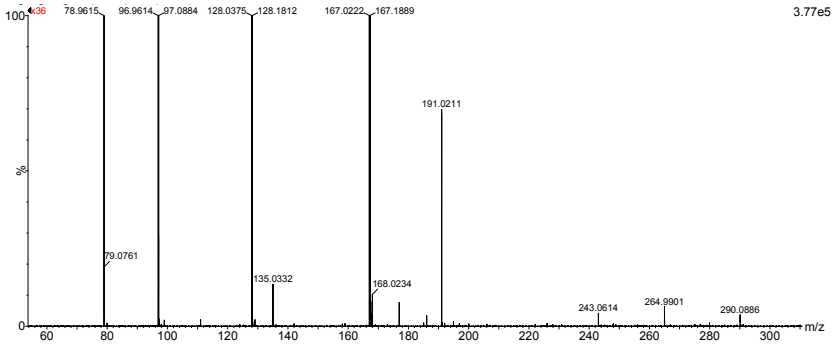

Fig. S23 MS fragmentation for the m/z 243.0614 (Peak **2**)

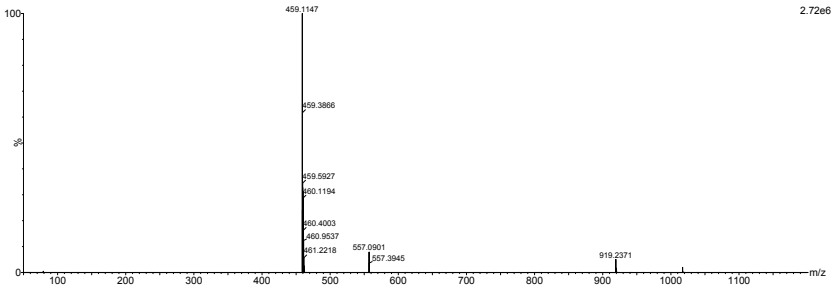

Fig. S24 MS fragmentation for the m/z 459.1147 (Peak **11**)

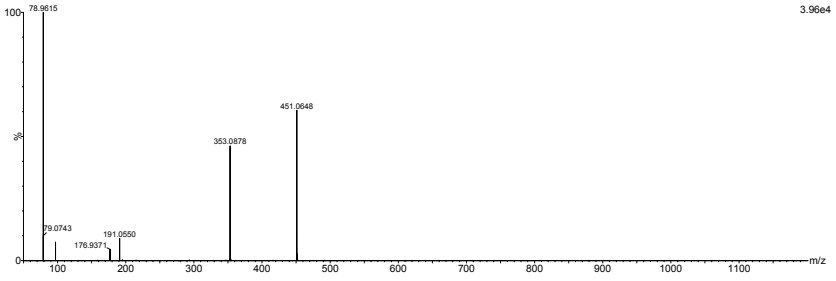

Fig. S25 MS fragmentation for the m/z 353.0878 (Peak **41**)

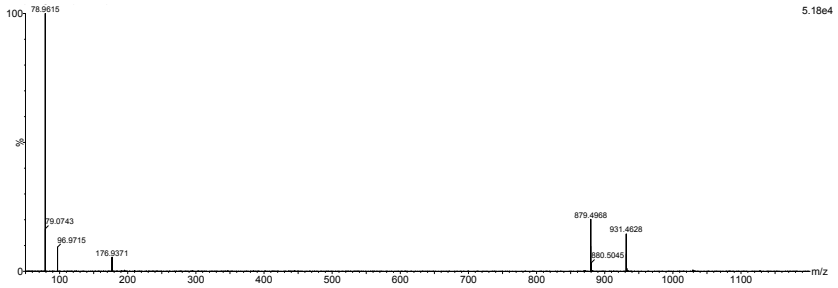

Fig. S26 MS fragmentation for the m/z 879.4968 (Peak **14**)

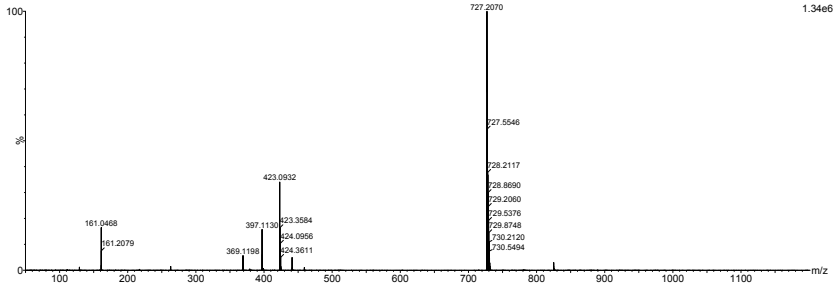

Fig. S27 MS fragmentation for the m/z 727.2070 (Peak **15**)

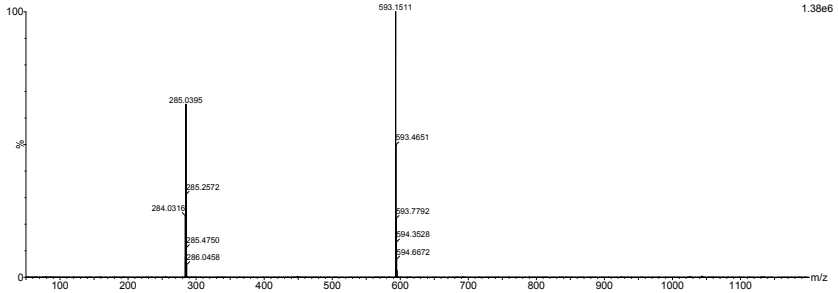

Fig. S28 MS fragmentation for the m/z 593.1511/595.1666 (Peak **16**)

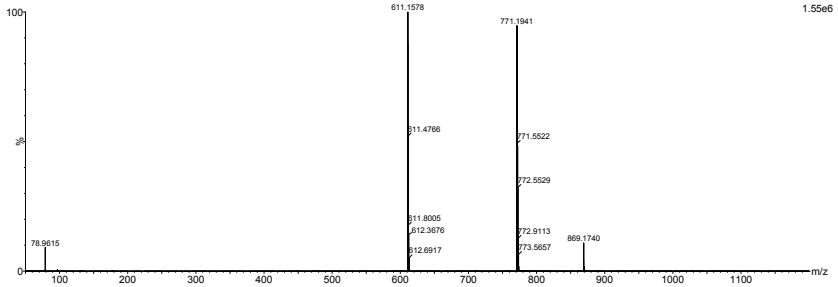

Fig. S29 MS fragmentation for the m/z 771.1941/773.2084 (Peak **47**)

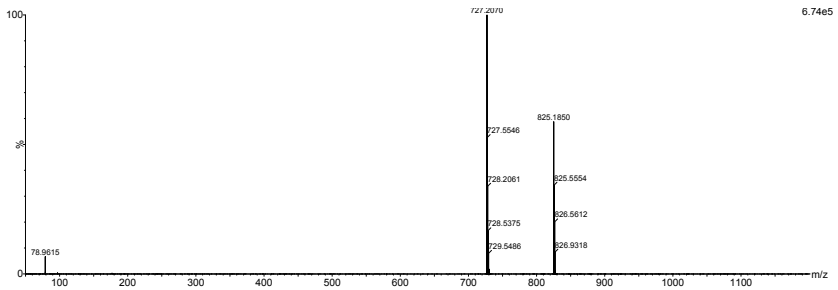

Fig. S30 MS fragmentation for the m/z 727.2070 (Peak **45**)

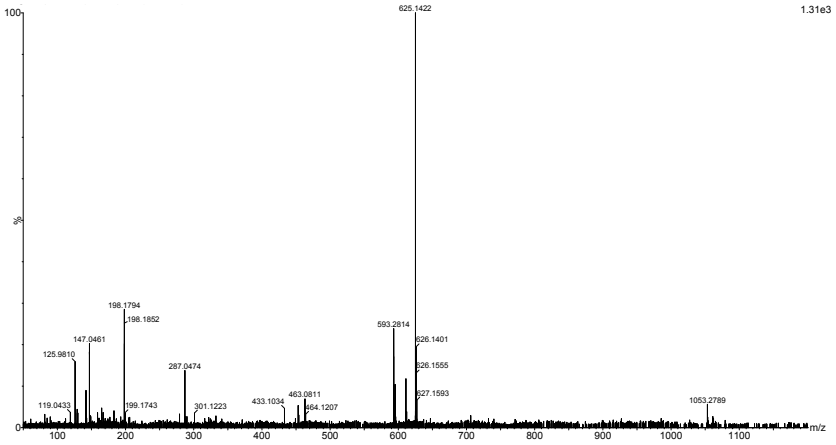

Fig. S31 MS fragmentation for the m/z 625.1422 (Peak **17**)

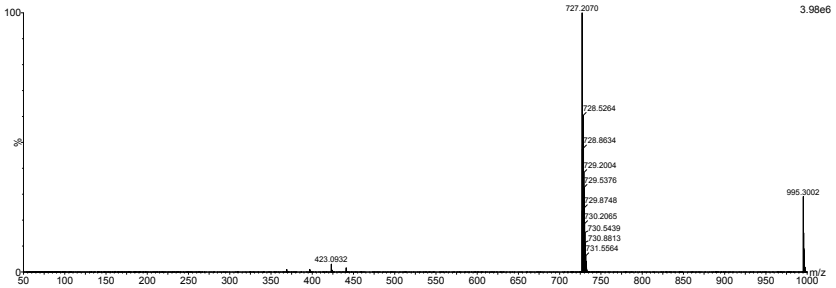

Fig. S32 MS fragmentation for the m/z 995.3002 (Peak **19**)

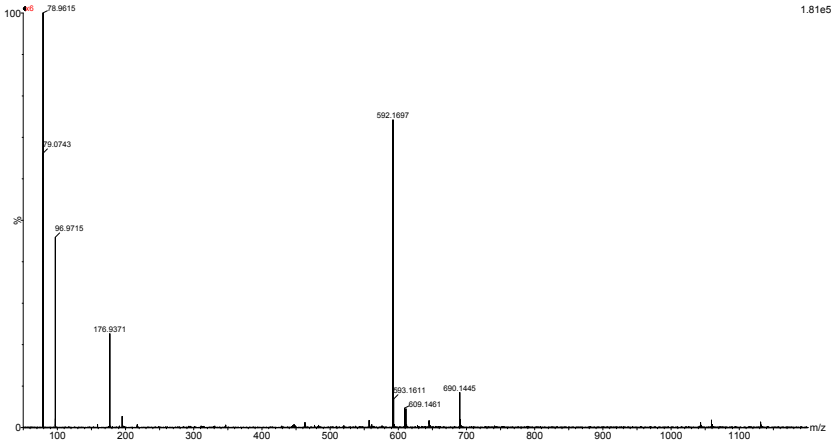

Fig. S33 MS fragmentation for the m/z 592.1697 (Peak **20**)

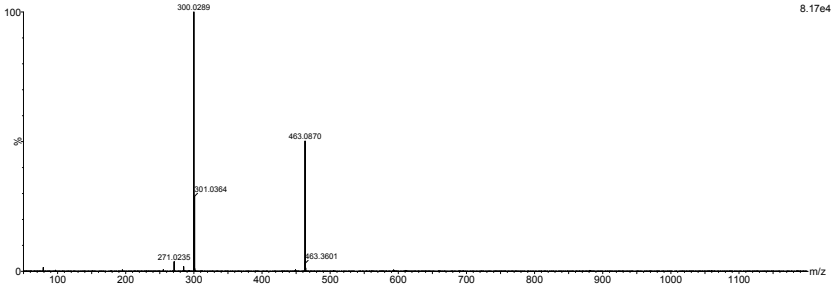

Fig. S34 MS fragmentation for the m/z 463.0870/465.1041 (Peak **42**)

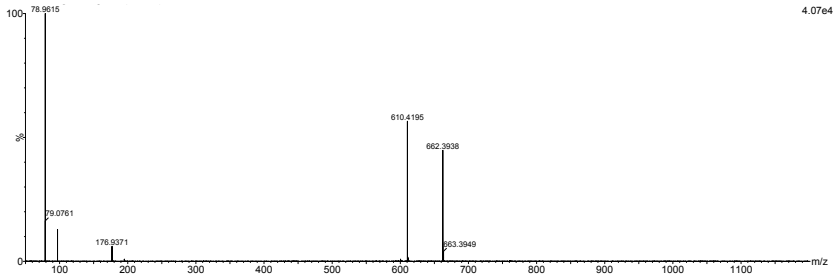

Fig. S35 MS fragmentation for the m/z 663.3949 (Peak **21**)

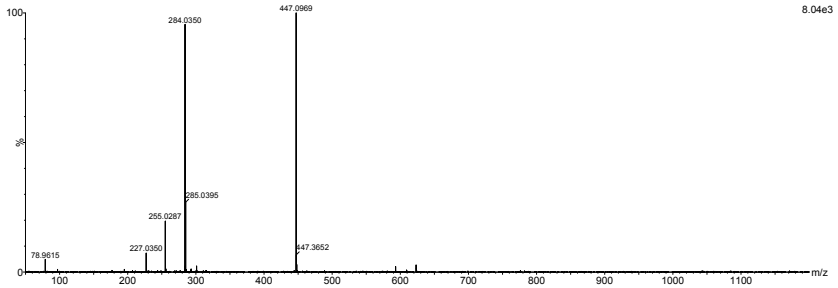

Fig. S36 MS fragmentation for the m/z 447.0969 (Peak **22**)

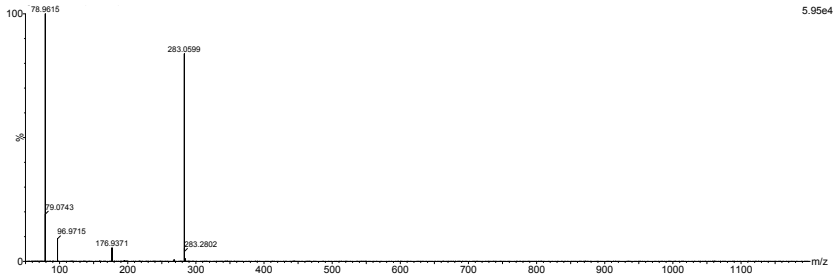

Fig. S37 MS fragmentation for the m/z 283.0599/285.0750 (Peak **23**)

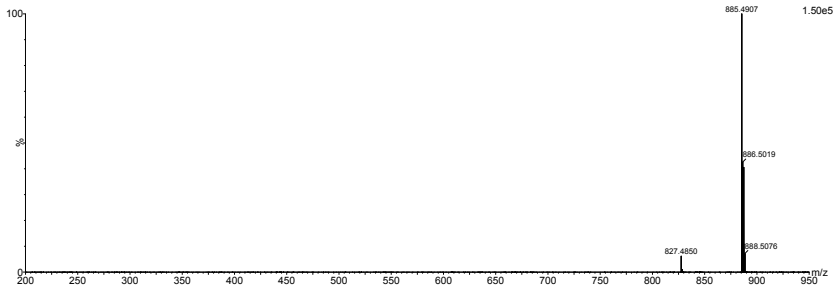

Fig. S38 MS fragmentation for the m/z 885.4907 (Peak **25**)

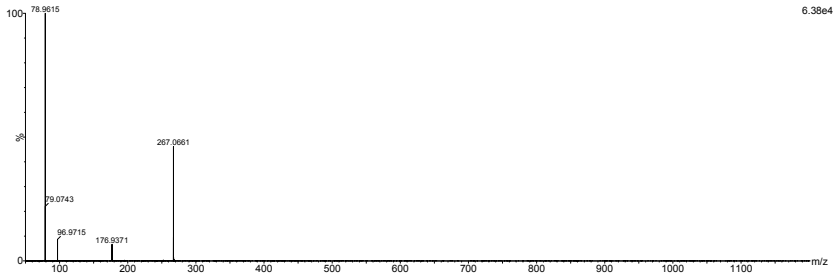

Fig. S39 MS fragmentation for the m/z 267.0661/269.0810 (Peak **26**)

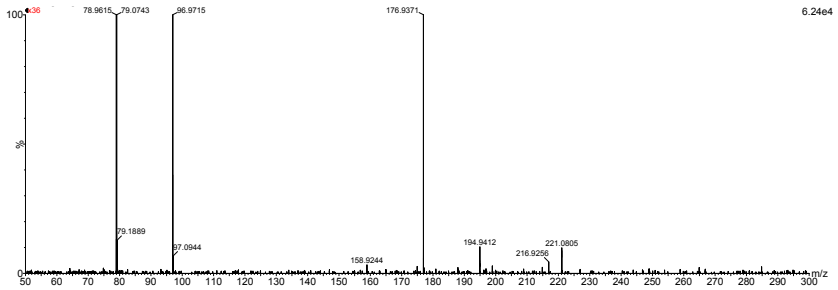

Fig. S40 MS fragmentation for the m/z 221.0805 (Peak **46**)

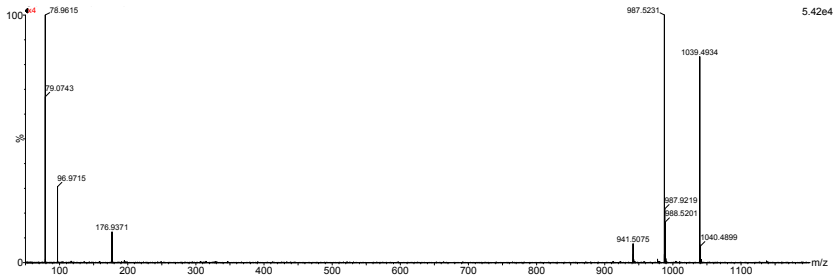

Fig. S41 MS fragmentation for the m/z 987.5231 (Peak **29**)

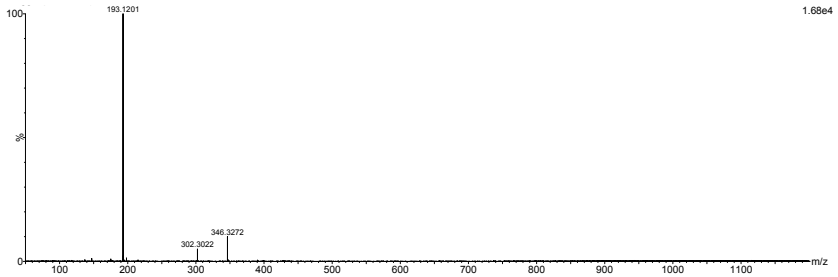

Fig. S42 MS fragmentation for the m/z 193.1201 (Peak **44**)

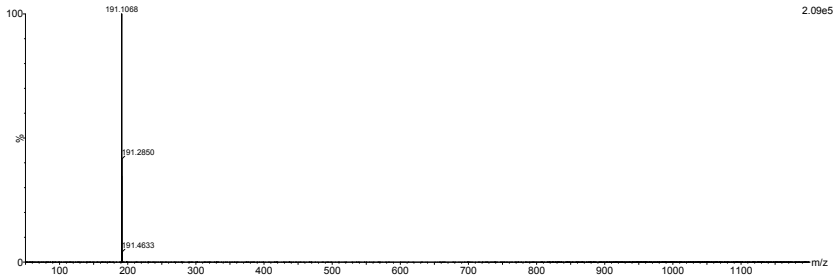

Fig. S43 MS fragmentation for the m/z 191.1068 (Peak **31**)

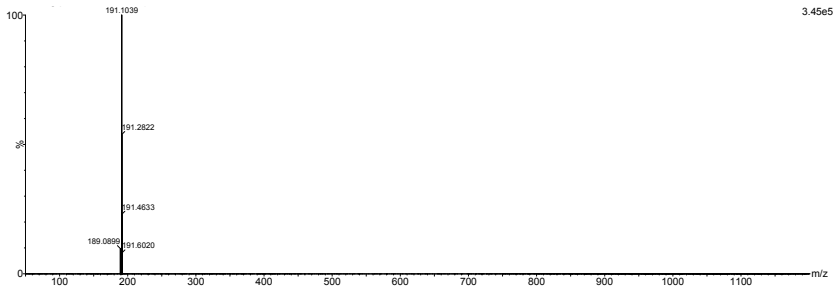

Fig. S44 MS fragmentation for the m/z 189.0899 (Peak **32**)

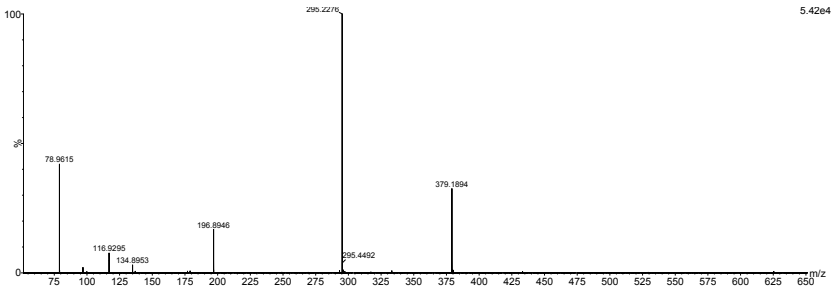

Fig. S45 MS fragmentation for the m/z 379.1894 (Peak **33**)

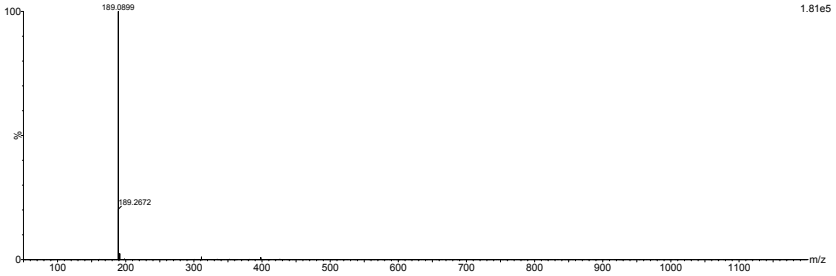

Fig. S46 MS fragmentation for the m/z 189.0899 (Peak **34**)

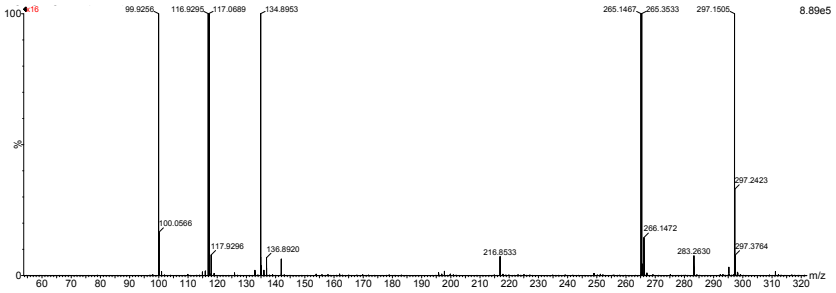

Fig. S47 MS fragmentation for the m/z 283.2630 (Peak **35**)

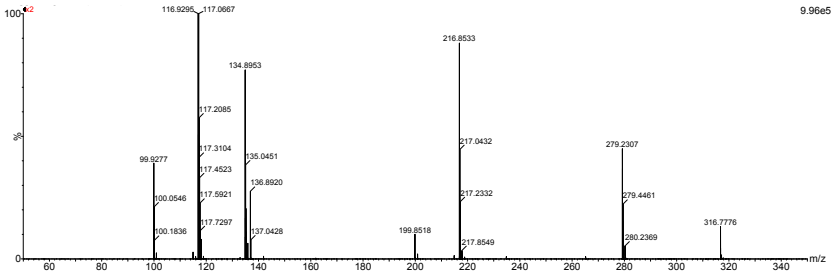

Fig. S48 MS fragmentation for the m/z 279.2307 (Peak **38**)

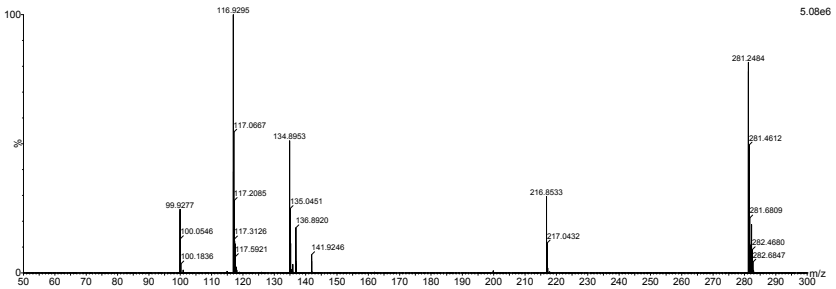

Fig. S49 MS fragmentation for the m/z 281.2484 (Peak **39**)